

# blood

Prepublished online February 21, 2008;  
doi:10.1182/blood-2007-12-129833

## **Targeting Bcl-2 family members with the BH3 mimetic AT-101 markedly enhances the therapeutic effects of chemotherapeutic agents in in vitro and in vivo models of B-cell lymphoma**

Luca Paoluzzi, Mithat Gonen, Jeffrey R Gardner, Jill Mastrella, Dajun Yang, Jon Holmlund, Mel Sorensen, Lance Leopold, Katia Manova, Guido Marcucci, Mark L Heaney and Owen A O' Connor

Articles on similar topics can be found in the following Blood collections

[Apoptosis](#) (746 articles)

[Neoplasia](#) (4217 articles)

---

Information about reproducing this article in parts or in its entirety may be found online at:  
[http://bloodjournal.hematologylibrary.org/site/misc/rights.xhtml#repub\\_requests](http://bloodjournal.hematologylibrary.org/site/misc/rights.xhtml#repub_requests)

Information about ordering reprints may be found online at:  
<http://bloodjournal.hematologylibrary.org/site/misc/rights.xhtml#reprints>

Information about subscriptions and ASH membership may be found online at:  
<http://bloodjournal.hematologylibrary.org/site/subscriptions/index.xhtml>

---

Advance online articles have been peer reviewed and accepted for publication but have not yet appeared in the paper journal (edited, typeset versions may be posted when available prior to final publication). Advance online articles are citable and establish publication priority; they are indexed by PubMed from initial publication. Citations to Advance online articles must include the digital object identifier (DOIs) and date of initial publication.

Blood (print ISSN 0006-4971, online ISSN 1528-0020), is published weekly by the American Society of Hematology, 2021 L St, NW, Suite 900, Washington DC 20036.

Copyright 2011 by The American Society of Hematology; all rights reserved.



## **Targeting Bcl-2 Family Members with the BH3 Mimetic AT-101 Markedly Enhances the Therapeutic Effects of Chemotherapeutic Agents in In Vitro and In Vivo Models of B-Cell Lymphoma**

Luca Paoluzzi<sup>1</sup>, Mithat Gonen<sup>3</sup>, Jeffrey R. Gardner<sup>4</sup>, Jill Mastrella<sup>1</sup>, Dajun Yang<sup>5</sup>, Jon Holmlund<sup>5</sup>, Mel Sorensen<sup>5</sup>, Lance Leopold<sup>5</sup>, Katia Manova<sup>6</sup>, Guido Marcucci<sup>7</sup>, Mark L. Heaney<sup>4</sup>, Owen A. O'Connor<sup>1,2\*</sup>.

<sup>1</sup>Herbert Irving Comprehensive Cancer Center, <sup>2</sup>College of Physician and Surgeons, Columbia University, N.Y., N.Y.; <sup>3</sup>Department of Epidemiology & Biostatistics, <sup>4</sup>Department of Medicine, <sup>6</sup>Molecular Cytology Core Facility, Memorial Sloan-Kettering Cancer Center, N. Y., NY ; <sup>5</sup>Ascenta Therapeutics, CA, <sup>7</sup>Division of Hematology/Oncology, The Ohio State University.

### **\* Corresponding Author**

#### **All correspondence should be addressed to:**

Owen A. O'Connor, M.D., Ph.D.  
Lymphoid Development and Malignancy Program  
Herbert Irving Comprehensive Cancer Center  
Columbia University  
1130 St. Nicholas Avenue  
New York, N.Y. 10032  
Phone: 212-851-4701  
Fax: 212-851-4710  
oo2130@columbia.edu

## ABSTRACT

Over-expression of anti-apoptotic members of the Bcl-2 family are observed in approximately 80% of B-cell lymphomas, contributing to intrinsic and acquired drug resistance. Nullifying anti-apoptotic function can potentially overcome this intrinsic and acquired drug resistance. AT-101 is a BH3 mimetic known to be a potent inhibitor of anti-apoptotic Bcl-2 family members including Bcl-2, Bcl- $X_L$  and Mcl-1. In vitro, AT-101 exhibits concentration and time dependent cytotoxicity against lymphoma and multiple myeloma cell lines, enhancing the activity of cytotoxic agents. The  $IC_{50}$  for AT-101 is between 1 and 10  $\mu$ M for a diverse panel of B-cell lymphomas. AT-101 was synergistic with carfilzomib (C), etoposide (E), doxorubicin (D) and 4-hydroxycyclophosphamide (4-HC) in mantle cell lymphoma (MCL) lines. In a transformed large B-cell lymphoma line (RL), AT-101 was synergistic when sequentially combined with 4-HC, but not when both drugs were added simultaneously. AT-101 also induced potent mitochondrial membrane depolarization ( $\Delta\Psi_m$ ) and apoptosis when combined with carfilzomib, but not with bortezomib in MCL. In SCID beige mouse models of drug resistant B-cell lymphoma, 35 mg/kg/day of AT-101 was safe and efficacious. The addition of AT-101 to cyclophosphamide (Cy) and rituximab (R) in a schedule-dependent manner enhanced the efficacy of the conventional therapy.

## INTRODUCTION

Bcl-2 and related proteins are key regulators of apoptosis that are expressed in solid tumors and hematologic malignancies<sup>1</sup>. Bcl-2 is known to be constitutively over-expressed in approximately 80% of follicular lymphomas and 20% of diffuse B-cell lymphomas as a result of the t(14; 18) translocation and gene amplification, respectively.<sup>2,3</sup> Over-expression of anti-apoptotic family members is associated with inhibition of apoptosis and chemotherapy resistance, resulting in lower clinical response rates and shortened survivals.<sup>4-9</sup> Targeting Bcl-2 family members offers new opportunities to address these survival pathways directly. One important benefit of these drugs relates to their ability to lower the threshold required to induce apoptosis, making them potentially complimentary with conventional chemotherapy approaches.

AT-101, a derivative of the natural product gossypol, is a BH3 mimetic capable of binding to Bcl-2, Bcl-X<sub>L</sub> and Mcl-1, attenuating their anti-apoptotic influence.<sup>10</sup> Gossypol is a natural compound extracted from cottonseeds (*Gossypium* sp.), which was initially used as an anti-fertility agent<sup>11</sup> and subsequently as a cytotoxic agent.<sup>12-20</sup> In the late 1980s, it was discovered that (-)-gossypol enantiomer exhibited the most potent anticancer activity compared to the racemic mixture or the (+)-gossypol enantiomer. The 3D solution structure of small molecules including (-)-gossypol in complex with Bcl-X<sub>L</sub> revealed several crucial interactions accounting for the binding specificity of the negative enantiomer. Given the importance of Bcl-2 over-expression in many types of lymphoma, we investigated the in vitro and in vivo antitumor activity of AT-101 alone and in combination with different cytotoxic and biological agents. The major objective of these studies was to define the best strategy for combining AT-101 with other agents based upon an understanding of its biological effects on the cell.

## **MATERIALS AND METHODS**

### **Cells and cell lines**

RL is an EBV-negative diffuse large B-cell lymphoma line (DLBCL) harboring the t(14; 18) translocation; H9 is a cutaneous T-cell lymphoma (CTCL) line obtained from ATCC (Manassas, VA); SKI is a diffuse large B-cell lymphoma line;<sup>21, 22</sup> HBL-2 and Granta are mantle cell lymphoma lines and both stain positive for Bcl-2;<sup>23,24</sup> JJN-3 is a multiple myeloma cell line.<sup>25</sup> All cell lines were grown as previously described.<sup>26</sup>

### **Materials**

All reagents for western blotting were obtained from Bio-Rad Laboratories (Hercules, CA) and Pierce Biotechnology, Inc. (Rockford, IL); dimethyl sulfoxide (DMSO) was obtained from Sigma (St. Louis, MO). Drugs were obtained as follows: AT-101 from Ascenta Therapeutics, Inc. (San Diego, CA); 4-Hydroxycyclophosphamide from Niomech (Bielefeld, Germany); carfilzomib from Proteolix (South San Francisco, CA) while all other drugs were obtained from the research pharmacy.

### **Cytotoxicity assays**

For all in vitro assays, cells were counted and re-suspended at an approximate concentration of  $3 \times 10^5$  cells / well in a 24-well plate (Becton Dickinson Labware, Franklin Lakes, NJ). AT-101 was diluted in DMSO which was maintained at a final concentration of less than 0.5%. Concentrations of AT-101 from 1 nM to 10  $\mu$ M were used in most experiments. Following incubation at 37°C in a 5% CO<sub>2</sub> humidified incubator, 100  $\mu$ L from each well was transferred to a 96 well opaque-walled plate; cell-Titer-Glo Reagent (Promega Corporation, Madison, WI) was

added in a 1:1 ratio. Contents were mixed for 2 minutes on an orbital shaker to induce cell lysis. The plates were allowed to incubate at room temperature for 10 minutes before recording luminescence with a Synergy™ HT Multi-Detection Microplate Reader (Biotek Instruments, Inc., Winooski, VT). In the schedule dependency experiments, serial dilutions of each drug were prepared in ratios relative to their IC<sub>50</sub>. Cells were pre-incubated with AT-101 for up to 72 hours while 4-HC was added for a 24 hour period, being added at time 0, 24 hours, and 48 hours from the start of incubation. Each experiment was performed in triplicate and repeated at least twice.

### **Flow cytometry**

RL or HBL-2 cells were seeded at a density of  $7 \times 10^5$ /mL. For the transmembrane mitochondrial membrane potential ( $\Delta\psi_m$ ) determination, cells were incubated with concentrations of AT-101 from 1 nM to 10  $\mu$ M for up to 24 hours, stained with 1.3  $\mu$ g/mL of the JC-1 dye (Invitrogen, Carlsbad, CA) for 30 min and incubated at 37° in normal growth media, then washed once in PBS, re-suspended in a 200  $\mu$ L of media and analyzed using a FACSCalibur Flow Cytometer (BD, Franklin Lakes, NJ). A minimum of  $5 \times 10^4$  / mL events were acquired from each sample. The green and red fluorescence intensities were resolved by detection in the FL1 and FL2 channels respectively. Median values obtained from the gated FL1 and FL2 channels were used to calculate the normalized transmembrane mitochondrial membrane potential ( $\Delta\psi_m$ ). Each experiment was performed in triplicate. Data are presented as the average  $\pm$  standard deviation (SD). For detection of apoptosis, Yo-Pro-1 and propidium iodide (PI) were used (Vybrant apoptosis assay kit #4, Invitrogen, Carlsbad, CA). After incubation with the approximate IC<sub>10-30</sub> of AT -101 alone and in combination with the approximate IC<sub>10-30</sub> of bortezomib or carfilzomib for 24 hours, cells were washed in cold PBS, centrifuged and re-suspended in PBS. One microliter of Yo-Pro-1 and 1  $\mu$ L of PI were added to each 1 mL of cell suspension. The fluorescence

signals acquired by a FACSCalibur System were resolved by detection in the conventional FL1 and FL3 channels. Cells were considered early apoptotic if Yo-Pro-1 positive but PI negative, late apoptotic if Yo-Pro-1 and PI positive.

### **Bcl-2 immunoblotting**

RL cells were seeded at a density of  $7 \times 10^5$ /mL and incubated with AT-101 at 100 nM, 1  $\mu$ M or 10  $\mu$ M under normal growth conditions for 8 or 24 hours. Bcl-2 immunoblotting experiments were performed as described previously <sup>26</sup>.

### **Confocal microscopy analysis**

Cells were seeded at a density of  $7 \times 10^5$ /mL. After incubation with AT-101 at 10  $\mu$ M for 24h, cells were exposed to 5  $\mu$ g/mL Hoechst 33342, 5  $\mu$ g/mL MitoTracker Red and 1  $\mu$ g/mL YO-PRO-1 for 20' at room temperature. The membranes of apoptotic cells, but not the membranes of live cells, are permeable to the YO-PRO-1; Hoechst 33342 is a specific stain for AT-rich regions of double-stranded DNA, while MitoTracker Red is concentrated by active mitochondria in living cells. Fluorescence of stained cells was detected with the use of a laser scanning confocal microscope (Leica TCS AOBS SP2, inverted stand, Leica Microsystems Inc.). Image acquisition and analysis were performed with a semi-automated and design-based stereology system (MetaMorph version 6, Universal Imaging Corp., Downingtown, PA). The percentage of apoptotic cells (apoptotic ratio, AR) was calculated using the formula  $AR = A/T$  where A = apoptotic cells (YO-PRO-1- green positive plus Hoechst 33342- blue positive but MitoTracker-red negative cells) and T = total cell (Hoechst positive) count. Up to twenty images for each sample were acquired and analyzed in two different experiments.

## **Mouse xenograft models**

In vivo experiments were performed as described previously.<sup>26</sup> In brief, five- to 7-week-old severe combined immunodeficiency (SCID) beige mice (Taconic Laboratories, Germantown, NY) were injected with  $1 \times 10^7$  RL-DLBCL cells on the flank via a s.c. route. When tumor volumes approached  $50 \text{ mm}^3$ , mice were separated into treatment groups of eight to ten mice each. Tumors were assessed using the two largest perpendicular axes (l, length; w, width) as measured with standard calipers. Tumor volume was calculated using the formula  $\frac{4}{3} \pi r^3$ , where  $r = (l + w) / 4$ . Tumor-bearing mice were assessed for weight loss and tumor volume at least twice weekly. Animals were sacrificed when one-dimensional tumor diameter exceeded 2.0 cm, or after loss of >10% body weight in accordance with institutional guidelines. All studies were conducted under an approved institutional animal protocol. AT-101 was given by oral gavage (PO). Single agent experiments were conducted using AT-101 on the following doses and schedules: 25, 35, 50, 75, 100 mg/kg/day for up to 4 consecutive weeks; 200, 240, 280 mg/kg/week for up to 3 weeks; and 100, 120 and 140mg/kg on days 1, 4, 8, 11 on a 21-day cycle. In the combination experiments, AT-101 was administered at a dose of 35 mg/kg/day for 10 days or 200 mg/kg on days 0 and 6; rituximab (R, 10 mg/kg) and cyclophosphamide (Cy, 50 mg/kg) were administered by intraperitoneal (IP) injection on days 2, 4, 6, 8. For the in vivo experiments, AT-101 was prepared in a vehicle solution of 0.5% sodium carboxymethylcellulose (CMC, Sigma-Aldrich, St Louis, MO) dissolved in purified sterile water. Control groups were treated with the vehicle solution administered by oral gavage.

## **Plasma Pharmacokinetic Analyses**

Twenty non-tumor bearing SCID beige mice received either 35 mg/kg or 200 mg/kg AT-101 in a single dose by oral gavage. Blood collection was performed by intra-cardiac puncture before the



administration of AT-101 and after 30 minutes, 1.5 hours (hrs), 3 hrs, 6 hrs, 12 hrs and 24 hrs with up to 4 mice at each time point. Blood samples were collected in K<sub>2</sub>EDTA tubes (BD Vacutainer®, Franklin Lakes, NJ) and immediately placed in an ice bath. Within a maximum of 30 minutes following blood collection, centrifugation of blood samples at 3000 rpm for 5 min at 4°C was applied. Plasma was then transferred into a separate tube. Reduced glutathione (Roche Pharmaceuticals, Nutley, NJ) was added to the whole blood and plasma samples in order to achieve a concentration between 10nM and 20nM. The plasma concentrations of AT-101 in mouse plasma were measured using an electrospray LC/MS/MS assay (Micromass Quattro-LC triple quadrupole mass spectrometer, Agilent). The LC/MS/MS assay quantitation range was 20 to 2000 ng/mL based on ex vivo spiking of AT-101 in mouse plasma at an assay volume of 100 µL. The quantitation of AT-101 in mouse plasma was based on an internal standard approach of spiking internal standard at a constant level to all samples.

### **Statistical Analysis**

Tumor volume is presented graphically as the mean at each time point for each treatment group. Each animal's time-tumor volume curve is represented using the area under the curve (AUC) which is interpreted as the total tumor burden of the animal. A logarithmic transformation to normalize the AUC is followed by an analysis of variance for group comparisons with an adjustment for multiple comparisons using re-sampling. All significance testing is done at the  $p < 0.05$  level protecting the family wise error rate. For different in vitro experimental groups, permutation tests were performed to determine if any of the experimental groups was superior to a control group. The analysis compares groups using analysis of variance after a normalizing transformation. All p-values are adjusted using Dunnett's method.<sup>27</sup> For each cell line, the IC<sub>50</sub> (inhibitory concentration of 50% of cells) and the drug to drug interactions in terms of

synergism, additivity or antagonism were computed using the Calcsyn software (Biosoft, Cambridge, UK, combination index (CI) < 1 defines synergism, CI = 1 additivity, CI > 1 antagonism).

## RESULTS

**AT-101 sensitizes mantle cell lymphoma and diffuse large B cell lymphoma to chemotherapy in vitro.** Figures 1 through 3 present the data for the mantle cell lymphoma cell lines, while Figures 4 through 6 present in vitro and in vivo data for the large B-cell lymphoma experiments. The IC<sub>50</sub> values for AT-101 across a panel of different lymphoproliferative malignancies, ranged from: 1.2 to 7.4  $\mu$ M after a 24 hour exposure; 0.7 to 3.9  $\mu$ M after 48 hour exposure; and 0.3 to 1.7  $\mu$ M after 72 hours. In general, the range of IC<sub>50</sub> values was relatively restricted, with the mantle cell lymphoma line HBL-2 being the most sensitive, and the multiple myeloma being the most resistant (Figure 1A). Figure 1B and C present the combination of AT-101 with carfilzomib or 4-HC. In the HBL2 and Granta cell line, the combination of AT-101 plus bortezomib for 24 hours revealed antagonism (CI range from 1.5 to 2.9) while AT-101 plus carfilzomib showed synergism (CI range 0.3 to 0.9). AT-101 plus etoposide, doxorubicin, or 4-HC showed mathematical synergy in both MCL lines (CI range from 0.3 to 0.9). The combination of AT-101 and 4-HC was synergistic only when the two drugs were given in sequence with a 24 or 48 hour pre-exposure to AT-101 (CI  $\leq$  0.8, Figure 4D). When both drugs were added simultaneously, antagonism was observed (CI range 1.2 – 2.7).

**AT-101 disrupts the  $\Delta\psi_m$  in a concentration and time-dependent manner in a diffuse large B-cell and in mantle cell lymphoma lines.**  $\Delta\psi_m$  antecedes cell death and is a potentially important early biomarker of apoptosis. Figure 4A depicts the time and dose dependent changes

in the normalized  $\Delta\psi_m$  when cells (RL) were exposed to 1  $\mu\text{M}$ , 3  $\mu\text{M}$  or 10  $\mu\text{M}$  AT-101 for 1, 4, 8, 12 and 24 hours. After 24 hours there was a clear concentration dependent reduction in the  $\Delta\psi_m$  (from  $1.11 \pm 0.0096$  at 1 $\mu\text{M}$ , to  $0.5 \pm 0.0133$  for 3  $\mu\text{M}$  to  $0.14 \pm 0.0007$  for 10 $\mu\text{M}$ ), with more than an 80% change in the mitochondrial membrane potential between the lowest and highest concentrations. Since earlier time points did not elicit a concentration-dependent response, the data in Figure 4A suggest that there may be a critical time of exposure, between 12 and 24 hours, for cells exposed to the higher concentrations of AT-101 (3 and 10  $\mu\text{M}$ ). A multiple comparison analysis revealed that there was a statistically significant difference in  $\Delta\psi_m$  that favors 10  $\mu\text{M}$  for 24 hours compared to all other scenarios ( $p < 0.0001$ ). These changes in membrane potential were not attributable to a reduction in Bcl-2. Figure 4C demonstrates that the levels of Bcl-2 in RL cells were not affected following exposure to AT-101 at 0.1, 1 or 10  $\mu\text{M}$ . No significant changes in Bcl-2 levels were observed after 8h or 24h of exposure compared to control.

In the MCL lines AT-101 induced a concentration dependent depolarization of the mitochondrial membrane with a decrease of the normalized  $\Delta\psi_m$  of more than 50% in the range of 1-2  $\mu\text{M}$  for HBL-2 and 2-10  $\mu\text{M}$  for Granta (Figure 2A). The combination of AT-101 and 6 nM carfilzomib produced a significant decrease in  $\Delta\psi_m$  for the combinations compared to any single agent exposure (Granta:  $p = 0.0036$  and  $p = 0.0021$  for the comparisons to carfilzomib alone and AT-101 alone respectively; HBL-2:  $p = 0.0086$  and  $p = 0.0015$  for the same comparisons, Figure 2B and C). The combination of AT-101 and bortezomib did not elicit any significant change compared to bortezomib alone in both cell lines (data not shown).

### **AT-101 plus carfilzomib induces apoptosis in mantle cell lymphoma**

Treatment with AT-101 and carfilzomib for 24 hours induced apoptosis in both HBL-2 and Granta cell lines. Exposure of Granta cells to AT-101 plus carfilzomib induced apoptosis in more than 70% of cells, compared to only 20% for AT-101 alone ( $p=0.0006$ ) and approximately 45% for carfilzomib alone ( $p=0.0463$ , Figure 3A). When HBL-2 cells were treated with AT-101 and a slightly lower dose of carfilzomib, about 50 % of the cells detected were apoptotic, compared to less than 20% for the individual drugs ( $p=0.0131$  and  $p=0.0156$  for the comparisons to carfilzomib and AT-101 alone respectively, Figure 3B). When AT-101 was combined with bortezomib, significantly less apoptosis was observed in the combination group compared to bortezomib alone in both cell lines (Figure 3C and D).

### **Confocal microscopy shows induction of apoptosis in a large B-cell lymphoma line**

Confocal microscopy was used to directly study changes in the treated cell populations as a function of concentration and duration of exposure. The incubation of RL cells with 10  $\mu$ M AT-101 for 24 hours induced apoptosis based upon the YO-PRO-1, Hoechst 33342 and MitoTraker Red staining. Treated cells revealed an apoptotic ratio of 38.7% compared to a 3% in the untreated controls (Figure 4B). Cells exposed to AT-101 for 24 hours revealed a prevalence of both YO-PRO-1 and Hoechst 33342 positive and MitoTraker Red negative cells, likely representing a later phase of apoptosis. However, treatment of cells at lower concentrations or for shorter durations of exposure produced a minimal change in the YO-PRO-1 and Hoechst 33342 positive and MitoTraker positive cells. These data corroborate the in vitro studies and the  $\Delta\psi_m$  data supporting the finding that 10  $\mu$ M of AT-101 for 24 hours seems to be optimal in inducing apoptosis.

### **Single dose AT-101 plasma pharmacokinetics in SCID beige mice**

The AT-101 peak plasma concentration was observed after 30 minutes of administration of the drug by oral gavage at two dose levels (35 mg/kg and 200 mg/kg). The 200 mg/kg group demonstrated an average plasma concentration ( $C_{max}$  and AUC) almost four times greater than the 35 mg/kg group (with  $C_{max}$  at 27.78  $\mu$ M and 7.88  $\mu$ M respectively). Twenty-four hours after exposure to AT-101, drug was still detectable in the plasma with average concentrations of 0.49  $\mu$ M for the 35 mg/kg group and 0.39  $\mu$ M for the 200 mg/kg (Figure 5A).

### **In Vivo Activity of AT-101 Reveals Marginal Single Agent Activity but Marked Potentiation of Conventional Cytotoxic Therapy**

Early experiences with AT-101 in the in vivo models were directed toward understanding the toxicity and efficacy of various single agent schedules. The RL cell line was selected because of its known chemotherapy and AT-101 resistance. A variety of schedules were explored as described in Figure 5B. Overall, increasing the dose of AT-101 from 25 mg/kg to 100 mg/kg per day indefinitely resulted in earlier onset of weight loss equivalent to more than 10% of the pre-treatment weight and death in many animals. For example, mice receiving 75 or 100 mg/kg/day lost 10% of their body weight by days 14 and 7 respectively, with almost all animals dying from drug related toxicity by day 21 (four out of five) and day 16 (five out of five) respectively. Mice treated with 50, 75 or 100 mg/kg/day lost a statistically significant amount of weight (i.e. > 10% compared with control animals [ $p=0.029$ ,  $p=0.016$  and  $p=0.016$ ] respectively). A statistical analysis of weight changes as a function of time yielded area under the curve values correlating with cumulative weight loss (i.e. toxicity) as a function of different treatment groups. These data demonstrated that mice receiving: 25 mg/kg/day for up to four weeks; 35 mg/kg daily for two weeks; 200 mg/kg/weekly for three consecutive weeks and 100 mg/kg on days 1, 4, 8, 11 schedules lost some weight relative to control animals, although less than 10% of their

pretreatment weight. In another analysis, the time to death from drug related causes suggested a statistically significant advantage for the 25 mg/kg/day for four weeks schedule over any other cohort with a significantly shorter survival and greater toxicity being appreciated for the 240 mg/kg/week x 3 ( $p=0.016$ ), 280 mg/kg week x 3 ( $p=0.016$ ), 50 mg/kg/day x 14 days ( $p=0.029$ ), 75 mg/kg/day schedules ( $p=0.016$ ) and 100 mg/kg/day ( $p=0.016$ ) cohorts compared to control.

Interestingly, the assessment of tumor volume across all treatment cohorts revealed no statistically significant tumor shrinkage for AT-101 treated animals compared to the control, except for the cohort receiving 35 mg/kg/day for two weeks ( $p=0.008$ ). This latter cohort was the only one that demonstrated a statistically significant reduction in tumor schedule of all the schedules and doses studied. Figure 5B presents the tumor volume growth curves for these different treatment cohorts. Mice receiving 120 mg/m<sup>2</sup> on days 1, 4, 8 and 11, while trending toward a statistically significant therapeutic outcome, also experienced significant weight loss and toxicity on this schedule. Based on these toxicological experiments and the efficacy findings, 35 mg/kg/day was chosen for future combination experiments.

Combination experiments focused on integrating AT-101 with cyclophosphamide (C) and rituximab (R). Overall, these regimens were well tolerated. After eight days of treatment, mice receiving AT-101 alone, AT-101 + C and AT-101 + R + C showed an average weight loss of between 10% and 15% which recovered once treatment was stopped. Figure 6A presents the area under the curve of tumor growth as a function of time. These data demonstrate that no single agent displayed a therapeutic advantage versus the control, nor were the differences significantly better when compared to each other. In this experiment, intentionally lower doses and less dose intense schedules were employed in order to identify potentially favorable drug-drug interactions. Among the doublet comparisons, AT-101 + C and AT-101 + Rituximab were not significantly better than any other doublet ( $p=0.182$ ). Interestingly, R + C was statistically

better than AT-101 alone ( $p=0.0371$ ), rituximab alone ( $p=0.0047$ ), and control ( $p=0.0174$ ), but was not superior to C alone ( $p=0.154$ ). Despite the lower doses and less dose intensity, AT-101 clearly improved the treatment effects of rituximab and C ( $p=0.0341$ ). Results of the multiple comparison analysis are shown in Figure 6B.

An additional combination experiment with AT-101 plus R and C was performed in order to explore a slightly different schedule of AT-101. This experiment was designed to determine if higher concentrations of AT-101, leading to more significant changes in  $\Delta\psi_m$ , would be associated with improved therapeutic outcome in the AT-101 + C and AT-101 + R cohorts. In these experiments, two single high doses of AT-101 (200 mg/kg) were given on days 0 and 6, while the R and C were given as previously described. Approximately 45 days from treatment, the combination of AT-101 + R was significantly better when compared to AT-101 alone ( $p = 0.0436$ ), rituximab alone ( $p=0.0004$ ) and control ( $p=0.0037$ ). The combination of AT-101 plus C was also significantly better than AT-101 alone ( $p=0.0007$ ), C alone ( $p=0.0016$ ), the control ( $p<0.0001$ ), rituximab alone ( $p<0.0001$ ) and the combination of R + C ( $p=0.0370$ ). The multiple comparison analysis trended toward significant ( $p=0.0637$ ) for the comparison of AT-101 200 mg/kg + R + C versus R + C alone. This experiment appears to corroborate the in vitro findings, suggesting that a higher  $C_{max}$  type exposure around the time of the chemotherapy may be the optimal strategy for synergizing with conventional chemotherapy agents.

## DISCUSSION

Therapeutic strategies targeting Bcl-2 represent a promising prospect for treating many types of cancers. Given the prominent role Bcl-2 family members play in lymphoproliferative malignancies, there is a strong rationale for targeting these pathways. At present there are a number of different strategies for targeting both the intrinsic and extrinsic arms of these survival

pathways, including small molecules, antisense approaches and monoclonal antibodies<sup>28-31</sup>. One of the major questions regarding the potential clinical application of these compounds revolves around precisely how to exploit them in combination. Practically, there is little expectation that these compounds will ever emerge as prominent single agents for the treatment of any cancer. Their development path is likely to require their integration into conventional chemotherapy regimens. This approach will require a detailed understanding of how Bcl-2 targeted drugs impact the relevant biology, and how basic pharmacologic considerations affect the activity of the combination. In these experiments, the major objective was to understand the optimal concentrations, doses, and schedules of AT-101, a small molecule BH3 mimetic that binds to the BH3 domain of Bcl-2, Bcl-X<sub>L</sub> and Mcl-1.<sup>10, 32-34</sup>

Mohammad RM et al<sup>35</sup> demonstrated that (-)-gossypol (AT-101) is capable of overcoming acquired and intrinsic drug resistance to CHOP chemotherapy. Jazirehi et al.<sup>36</sup> have demonstrated that rituximab down-regulates Bcl-2 expression and Bcl-X<sub>L</sub> transcription in lymphoma cell lines, reinforcing its potential role as a “Bcl-2 directed” therapy. These studies however, did not explore how different doses and schedules of AT-101 affected important pharmacokinetic or pharmacodynamic endpoints, nor how to use this information to establish optimal combination strategies.

Duration of exposure was generally not a critical determinant of cytotoxicity. The cytotoxicity data corroborate the  $\Delta\psi$ m data which similarly established the importance of concentration as major determinant of cytotoxicity. These data support the finding that while AT-101 does not affect levels of Bcl-2, it does affect Bcl-2 function as measured by the  $\Delta\psi$ . The observed effect on the  $\Delta\psi$  was prominent after 24 hours of exposure in a concentration range between 1  $\mu$ M and 10  $\mu$ M, suggesting the possible existence of a threshold concentration necessary to trigger apoptosis.



In the mantle cell lines (HBL-2 and Granta), AT-101 showed a synergistic interaction when combined with the proteasome inhibitor carfilzomib,<sup>37,38</sup> doxorubicin, etoposide or 4-HC after a 24 hours exposure. The combination with carfilzomib also showed induction of apoptosis and mitochondrial membrane depolarization after 24 hours, with the combination being statistically superior to any single agent in both cell lines. Interestingly the combination of AT-101 with bortezomib showed antagonism in the cytotoxicity assays and significantly less induction of apoptosis in both cell lines. Kuhn et al recently demonstrated that carfilzomib was more potent than bortezomib in overcoming both primary and secondary resistance to bortezomib in both cell line models and clinical samples.<sup>36</sup> The authors speculate that the irreversible effect of carfilzomib on the proteasome and immunoproteasome subunits may partially explain this observation.

Xenograft experiments in SCID-beige mice with AT-101 alone showed that a daily dose lower than 50 mg/kg could be safely administered for up to 2 - 4 weeks. The 35 mg/kg/day for a two week schedule was safe, and was the only schedule shown to be statistically better than the control or any other treatment cohort ( $p=0.008$ , Figure 5B), although the analysis of time to death was not statistically significantly different between the 35 mg/kg/day and control cohorts ( $p=0.405$ ). The single agent in vivo dosing experiments suggest that efficacy is not necessarily a function of dose, but rather, schedule as well. For example, 35 mg/kg/day for two weeks delivered a cumulative dose of 490 mg/kg, while only about 80% of this cumulative dose was delivered with the 100 mg/kg on the 1, 4, 8, 11 schedule (400 mg/kg). While both schedules were safe and feasible, the latter schedule was not associated with any therapeutic benefit. A similar comparison can be applied to the 35 mg/kg x 14 day schedule and the 200 mg/kg x 3 weekly doses, in which the latter schedule is associated with a greater cumulative dose, although with little to no improvement in tumor shrinkage and survival compared to the daily schedule.

The combination in vitro data with AT-101 and 4-HC in RL support the hypothesis that a pre-exposure to AT-101 for up to 48 hours is necessary in order to sensitize this relatively drug resistant cell line to conventional chemotherapy. Using the most effective single agent schedule of AT-101, a multiple comparison analysis of combination studies with rituximab and cyclophosphamide demonstrated the superiority of the triplet combination with 35 mg/kg/day AT-101 for ten days, starting two days before the administration of the other drugs. Interestingly, complete responses and statistically significant differences in tumor volume shrinkage were only observed in animals receiving rituximab and C, with no additive benefit in those mice receiving AT-101 plus rituximab or AT-101 plus cyclophosphamide. This is in contrast to the in vivo experiment in which AT-101 was administered at a very high single exposure (200 mg/kg x two doses on days 0 and 6) in combination with rituximab and C, in which there were significant improvements in the AT-101 plus C and AT-101 plus rituximab combinations, with a trend toward statistical significance in mice treated with AT-101 plus rituximab and C ( $p=0.0637$ ). These data also demonstrated a statistically significant advantage for those mice treated with AT + C compared to R + C, suggesting AT-101 in combination with C exceeded the benefits of adding rituximab. While the contributions of rituximab in these models is likely to be underestimated given the immunocompromised nature of these animals, the data still support an important role for the addition of this drug to the regimen.

Hence, two major observations have emerged from the in vivo experiments: (1) a low daily dose of AT-101, in fact the only schedule shown to induce significant responses compared to control, complimented the activity of only the combination of R + C and not the individual treatments with R or C alone; and (2) higher dose schedules of AT-101 complimented treatments of R and C alone, and trended toward significance with the combination of R plus C. Obviously, each of these two different schedules is associated with markedly different pharmacokinetic

profiles, with the peak plasma concentrations of 7.88 and 27.78  $\mu\text{M}$  in the 35 mg/kg/day and 200 mg/kg x 2 schedules respectively, while the plasma concentrations in both cases were  $< 1 \mu\text{M}$  after 24 hours. These data suggest that the average plasma peak concentration for the 200 mg/kg schedule is almost four times higher than the low dose schedule. These PK parameters appear to be in line with the concentrations noted to induce cytotoxicity in vitro ( $\text{IC}_{50}$  values for RL in the range of 3-4  $\mu\text{M}$ ) and  $\Delta\psi$  in most cell lines (i.e. the greatest changes in  $\Delta\psi$  occur between 1-10  $\mu\text{M}$  for 12 to 24 hours).

One potential explanation for the differences between the low dose and high dose AT-101 schedules with chemotherapy may revolve around the potency of AT-101's ability to influence apoptotic priming. Practically, it is well recognized that combinations of drugs are more effective and efficacious in producing cell death compared to single agents. Assuming there is a relationship between the change in the  $\Delta\psi$  and a reduction in the threshold for induction of apoptosis, it is plausible that low dose AT-101 schedules may result in less change in the  $\Delta\psi$  compared to higher dose schedules, therefore requiring a greater "pro-apoptotic influence" (i.e. R + C) to induce cell death. Clearly, AT-101 compliments the combination of R + C when given on the daily schedule. The higher dose schedule produces greater change in the  $\Delta\psi$ , therefore allowing induction of apoptosis with a relatively less toxic approach, as is seen with the 200 mg/kg dosing schedule with rituximab or C alone. Perhaps most importantly, these data suggest that there may be two different strategies to exploit the therapeutic advantage of AT-101, depending upon whether it is to be used as a single agent (daily) or in combination (weekly or pulse high dose). Future strategies for combination studies should focus on achieving the highest doses possible (i.e. greatest changes in  $\Delta\psi$ ) for short periods of time, around the time of cytotoxic therapy administration.

Clearly, future clinical studies will need to explore the appropriate pharmacodynamic endpoints as a function of various pharmacokinetic parameters in order to determine the best strategies for integrating these agents into standard chemotherapy regimens. These data have formed the basis for planned clinical studies in lymphoma.

### **Acknowledgments:**

LP is partially supported by an American-Italian Cancer Foundation Fellowship. OAO is the recipient of the Leukemia and Lymphoma Society Scholar in Research Award. OAO would like to thank the Joseph Nusim Fund for Mantle Cell Lymphoma Research for their support. MH is supported by the Naomi Rosenfeld Research Fund. We would also like to thank Proteolix for their advice and supply of carfilzomib and Biopharmaceutical Research Inc for the pharmacokinetic analysis.

Conflict of Interest Disclosure: Luca Paoluzzi's salary was partially subsidized by a grant from Ascenta; Owen A. O'Connor receives research support from Millenium, Proteolix, and Ascenta; Dajun Yang, Jon Holmlund, Mel Sorensen and Lance Leopold are employees of Ascenta Therapeutics.

Author Contributions: Luca Paoluzzi designed and performed all presented experiments, interpreted data, and wrote the manuscript; Mithat Gonen did the statistical analysis; Jeffrey Gardner contributed by doing the flow cytometry; Jill Mastrella contributed with the cytotoxicity assays; Dajun Yang, Jon Homlund, Mel Sorensen and Lance Leopold provided expertise regarding the design of the pharmacokinetic and in vivo experiments; Katia Manova provided assistance with the laser confocal microscopy; Guido Marcucci provided assistance with Bcl-2 western blots; Mark Heaney provided input regarding experiments measuring the transmembrane mitochondrial potential; Owen A. O'Connor provided input regarding experimental design, interpretation of data, and editing of the final manuscript.

## REFERENCES

1. Kluck RM, Bossy-Wetzel E, Green DR, Newmeyer DD. The release of cytochrome c from mitochondria: a primary site for Bcl-2 regulation of apoptosis. *Science* 1997; 275: 1132–6.
2. Yang E, Korsmeyer SJ. Molecular thanatopsis: a discourse on the BCL2 family and cell death. *Blood* 1996; 88: 386–401.
3. Yunis JJ, Frizzera G, Oken MM, McKenna J, Theologides A, Arnesen M. Multiple recurrent genomic defects in follicular lymphoma. A possible model for cancer. *N Engl J Med*. 1987 Jan 8; 316 (2): 79-84.
4. Yang J, Liu X, Bhalla K, et al. Prevention of apoptosis by Bcl-2: release of cytochrome c from mitochondria blocked. *Science* 1997; 275: 1129–32.
5. Johnstone RW, Ruefli AA, Lowe SW. Apoptosis: a link between cancer genetics and chemotherapy. *Cell*. 2002 Jan 25; 108 (2): 153-64. Review.
6. Reed JC. Bcl-2 and the regulation of programmed cell death. *J Cell Biol* 1994; 124: 1–6.
7. Wang JL, Liu D, Zhang ZJ, et al. Structure-based discovery of an organic compound that binds Bcl-2 protein and induces apoptosis of tumor cells. *Proc Natl Acad Sci USA* 2000; 97: 7124–9.
8. Shangary S, Johnson DE. Peptides derived from BH3 domains of Bcl-2 family members: a comparative analysis of inhibition of Bcl-2, Bcl-x(L) and Bax oligomerization, induction of cytochrome c release, and activation of cell death. *Biochemistry* 2002; 41: 9485–95.
9. Reed JC. Dysregulation of apoptosis in cancer. *J Clin Oncol*; 1999 Sep;17(9):2941-53.

10. Wang G, Nikolovska-Coleska Z, Yang CY, et al. Structure-based design of potent small-molecule inhibitors of anti-apoptotic Bcl-2 proteins. *J Med Chem.* 2006 Oct 19;49(21):6139-42.
11. Wu D. An overview of the clinical pharmacology and therapeutic potential of gossypol as a male contraceptive agent and in gynaecological disease. *Drugs* 1989; 38: 333–41.
12. Tuszynski GP, Cossu G. Differential cytotoxic effect of gossypol on human melanoma, colon carcinoma, and other tissue culture cell lines. *Cancer Res* 1984; 44: 768–71.
13. Coyle T, Levante S, Shetler M, Winfield J. In vitro and in vivo cytotoxicity of gossypol against central nervous system tumor cell lines. *JNeurooncol* 1994; 19: 25–35.
14. Gilbert NE, O'Reilly JE, Chang CJ, Lin YC, Brueggemeier RW. Antiproliferative activity of gossypol and gossypolone on human breast cancer cells. *Life Sci* 1995; 57: 61–7.
15. Wang X, Wang J, Wong SC, et al. Cytotoxic effect of gossypol on colon carcinoma cells. *Life Sci* 2000; 67: 2663–71.
16. Zhang M, Liu H, Guo R, et al. Molecular mechanism of gossypol-induced cell growth inhibition and cell death of HT-29 human colon carcinoma cells. *Biochem Pharmacol* 2003; 66: 93–103.
17. Stein RC, Joseph AE, Matlin SA, Cunningham DC, Ford HT, Coombes RC. A preliminary clinical study of gossypol in advanced human cancer. *Cancer Chemother Pharmacol.* 1992; 30 (6): 480-2.
18. Flack MR, Pyle RG, Mullen NM, et al. Oral gossypol in the treatment of metastatic adrenal cancer. *J Clin Endocrinol Metab.* 1993 Apr; 76 (4): 1019-24.
19. Van Poznak, C., Seidman, A.D., Reidenberg, M.M., et al. Oral gossypol in the treatment of patients with refractory metastatic breast cancer: a phase I/II clinical trial. *Breast Cancer Res Treat.* 2001 Apr; 66 (3): 239-48.

20. Bushunow P, Reidenberg MM, Wasenko J, et al. Gossypol treatment of recurrent adult malignant gliomas. *J Neurooncol.* 1999 May; 43 (1): 79-86.
21. Goy A, Gilles F, Remache Y, et al. Establishment of a human cell line (SKI-DLCL-1) with a t(1;14)(q21;q32) translocation from the ascites of a patient with diffuse large cell lymphoma. *Leuk Lymphoma* 2001; 40: 419–23.
22. Gilles F, Goy A, Remache Y, Shue P, Zelenetz AD. MUC1 dysregulation as the consequence of a t(1;14)(q21;q32) translocation in an extranodal lymphoma. *Blood* 2000; 95: 2930–6.
23. De Leeuw RJ, Davies JJ, Rosenwald A, et al. Comprehensive whole genome array CGH profiling of mantle cell lymphoma model genomes. *Hum Mol Genet.* 2004 Sep 1; 13 (17): 1827-37. Epub 2004 Jun 30.
24. Abe M, Nozawa Y, Wakasa H, Ohno H, Fukuhara S. Characterization and comparison of two newly established Epstein-Barr virus-negative lymphoma B-cell lines. Surface markers, growth characteristics, cytogenetics, and transplantability. *Cancer.* 1988 Feb 1; 61 (3): 483-90.
25. Jackson N, Lowe J, Ball J, Bromidge E, Ling NR. Two new IgA1-kappa plasma cell leukaemia cell lines (JJN-1 & JJN-2) which proliferate in response to B cell stimulatory factor 2. *Clin Exp Immunol.* 1989 Jan; 75 (1): 93-9.
26. O'Connor OA, Smith EA, Toner LE, et al. The combination of the proteasome inhibitor bortezomib and the bcl-2 antisense molecule oblimersen sensitizes human B-cell lymphomas to cyclophosphamide. *Clin Cancer Res.* 2006 May 1; 12(9):2902-11.
27. Hockberg Y, Tamhane AC. *Multiple Comparison Procedures.* Wiley. New York, 1987; 1-450.

28. Klasa RJ, Bally MB, Ng R, Goldie JH, Gascoyne RD, Wong FM. Eradication of human non-Hodgkin's lymphoma in SCID mice by BCL-2 antisense oligonucleotides combined with low-dose cyclophosphamide. *Clin Cancer Res.* 2000 Jun; 6 (6): 2492-500.
29. Loomis R, Carbone R, Reiss M, Lacy J. Bcl-2 antisense (G3139, Genasense) enhances the in vitro and in vivo response of Epstein-Barr virus-associated lymphoproliferative disease to rituximab. *Clin Cancer Res.* 2003 May; 9 (5): 1931-9.
30. Ramanarayanan J, Hernandez-Ilizaliturri FJ, Chanan-Khan A, Czuczman MS. Pro-apoptotic therapy with the oligonucleotide Genasense (oblimersen sodium) targeting Bcl-2 protein expression enhances the biological anti-tumour activity of rituximab. *Br J Haematol.* 2004 Dec; 127 (5): 519-30.
31. Smith MR, Jin F, Joshi I. Enhanced efficacy of therapy with antisense BCL-2 oligonucleotides plus anti-CD20 monoclonal antibody in scid mouse/human lymphoma xenografts. *Mol Cancer Ther.* 2004 Dec; 3 (12): 1693-9.
32. Korsmeyer SJ. BCL-2 gene family and the regulation of programmed cell death. *Cancer Res.* 1999 Apr 1; 59 (7 Suppl): 1693s-1700s.
33. Letai A, Bassik MC, Walensky LD, Sorcinelli MD, Weiler S, Korsmeyer SJ. Distinct BH3 domains either sensitize or activate mitochondrial apoptosis, serving as prototype cancer therapeutics. *Cancer Cell* 2002; 2: 183-92.
34. Kitada S, Leone M, Sareth S, Zhai D, Reed JC, Pellecchia M. Discovery, characterization, and structure-activity relationships studies of proapoptotic polyphenols targeting B-cell lymphocyte/leukemia-2 proteins. *J Med Chem* 2003; 46: 4259-64.
35. Mohammad RM, Wang S, Aboukameel A, et al. Preclinical studies of a nonpeptidic small-molecule inhibitor of Bcl-2 and Bcl-X(L) [(-)-gossypol] against diffuse large cell lymphoma. *Mol Cancer Ther.* 2005 Jan; 4 (1):13-21.

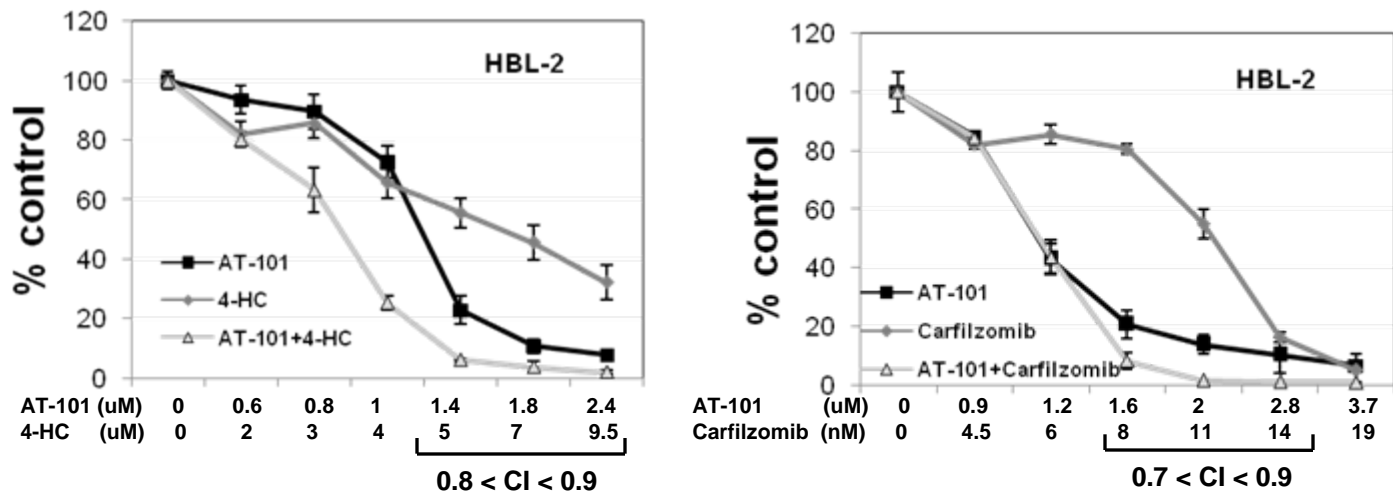


36. Jazirehi AR, Bonavida B. Cellular and molecular signal transduction pathways modulated by rituximab (rituxan, anti-CD20 mAb) in non-Hodgkin's lymphoma: implications in chemosensitization and therapeutic intervention. *Oncogene*. 2005 Mar 24; 24 (13): 2121-43.
37. Demo SD, Kirk CJ, Aujay MA, et al. Antitumor activity of PR-171, a novel irreversible inhibitor of the proteasome. *Cancer Res*. 2007 Jul 1;67(13):6383-91.
38. Kuhn DJ, Chen Q, Voorhees PM, et al. Potent activity of carfilzomib, a novel, irreversible inhibitor of the ubiquitin-proteasome pathway, against preclinical models of multiple myeloma. *Blood*. 2007 Nov 1;110(9):3281-90. Epub 2007 Jun 25.

A

	HBL-2	GRANTA	H9	RL	SKI	JJN-3
IC50 (μM) 24h	1.2 (0.5-1.6)	3.5 (1.9-6.3)	3.9 (2.3-6.4)	5.0 (3.0-8.0)	5.6 (3.1-9.8)	7.4 (5.6-9.6)
IC50 (μM) 48h	0.7 (0.5-0.9)	2.5 (2.2-2.8)	1.7 (0.9-3.2)	1.8 (1.3-2.7)	2.0 (1.2-3.4)	3.9 (2.5-6.0)
IC50 (μM) 72h	0.3 (0.2-0.5)	1.7 (1.3-2.1)	1.1 (0.4-2.7)	0.9 (0.6-1.4)	0.9 (0.4-1.8)	1.2 (0.8-1.8)

B



C

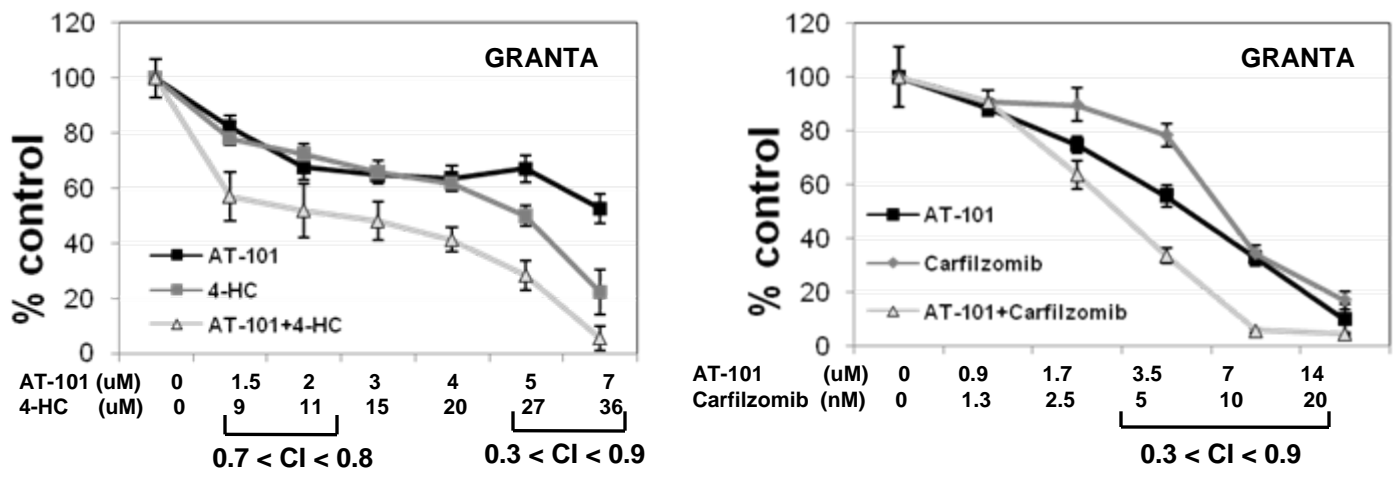


**Figure 1**  
**Luminometric assay (A)** AT-101 alone in 6 cell lines of lymphoma and multiple myeloma; IC50s (μM) to AT-101 are shown; confidence intervals are shown between parenthesis; **(B )** Combination of AT-101 with carfilzomib or 4-HC in HBL-2 after 24 hours. **(C)** Combination of AT-101 with carfilzomib or 4-HC in Granta after 24 hours.

A

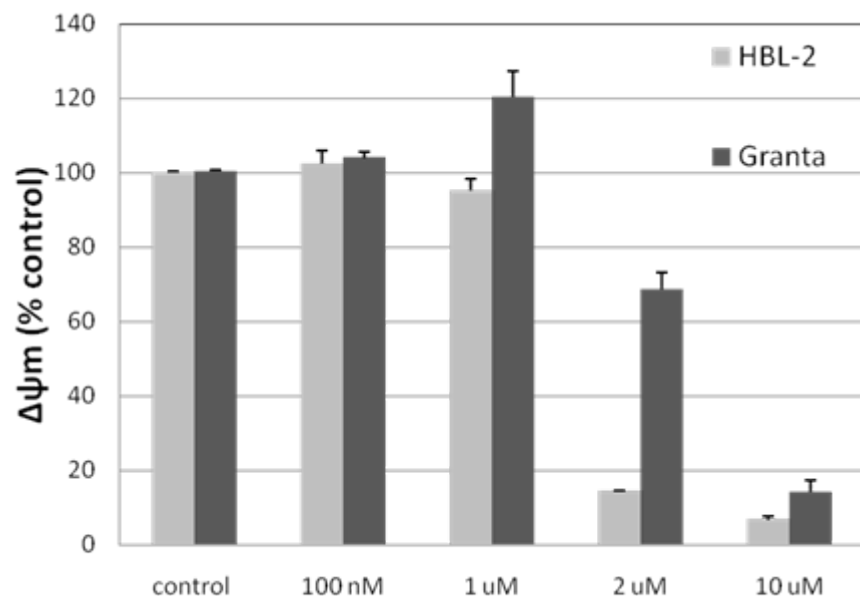
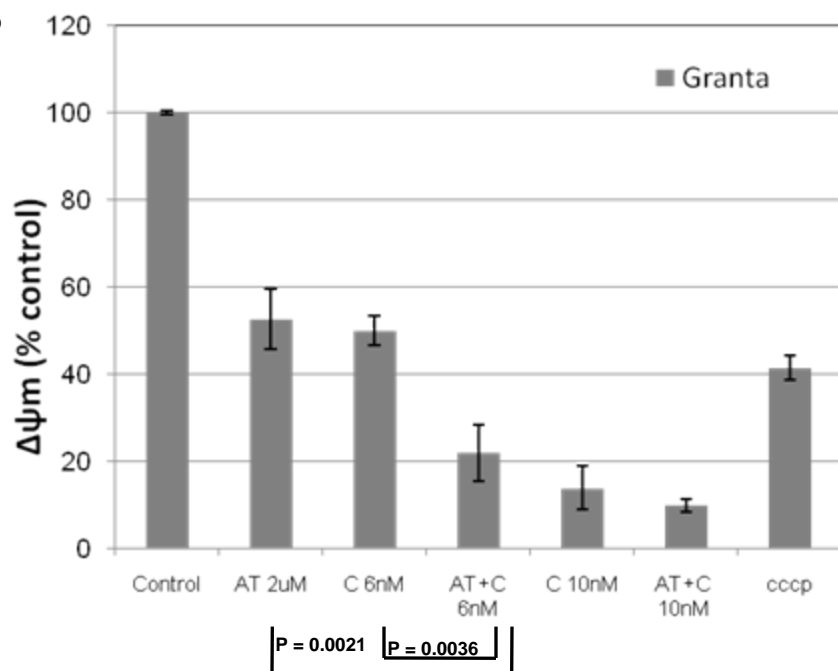
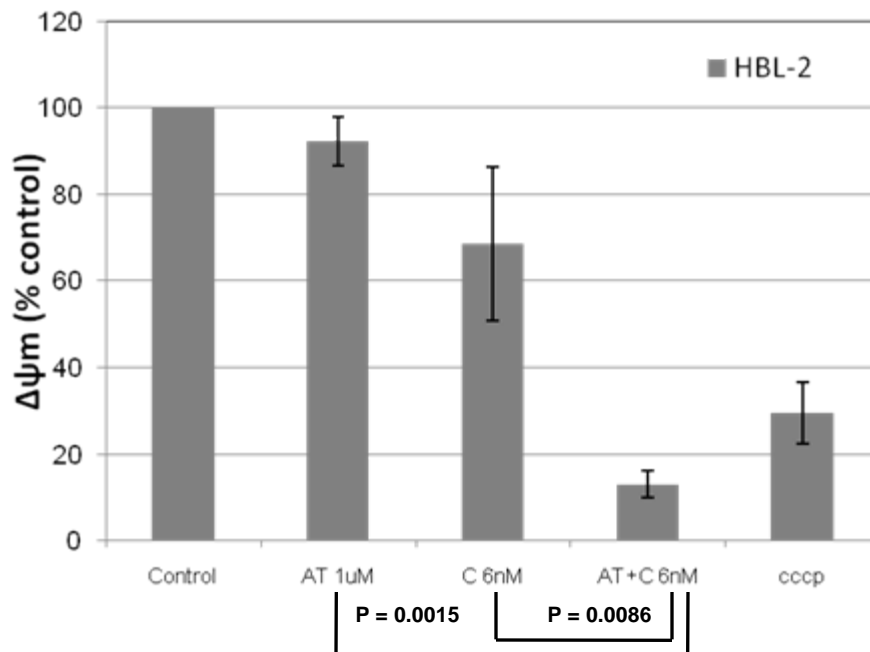


**Figure 2** Assessment of the mitochondrial membrane potential ( $\Delta\psi_m$ ) in HBL-2 and Granta (MCL). **(A)** HBL-2 and Granta cells were incubated with AT-101 from 100 nM to 10  $\mu$ M for 24h. **(B)** Granta cells were incubated with AT-101 (AT, 2  $\mu$ M) or carfilzomib (C, 6 or 10 nM) or both for 24h. The combination of AT-101 plus C at 6 nM was statistically significant compared to any of the single groups and controls ( $p \leq 0.0036$ ) **(C)** HBL-2 cells were incubated with AT-101 (AT, 1  $\mu$ M), carfilzomib (C, 6 nM) or for 24h. Again, the combination of AT-101 plus C was statistically significant compared to any of the single groups and controls ( $p \leq 0.0086$ )

B



C



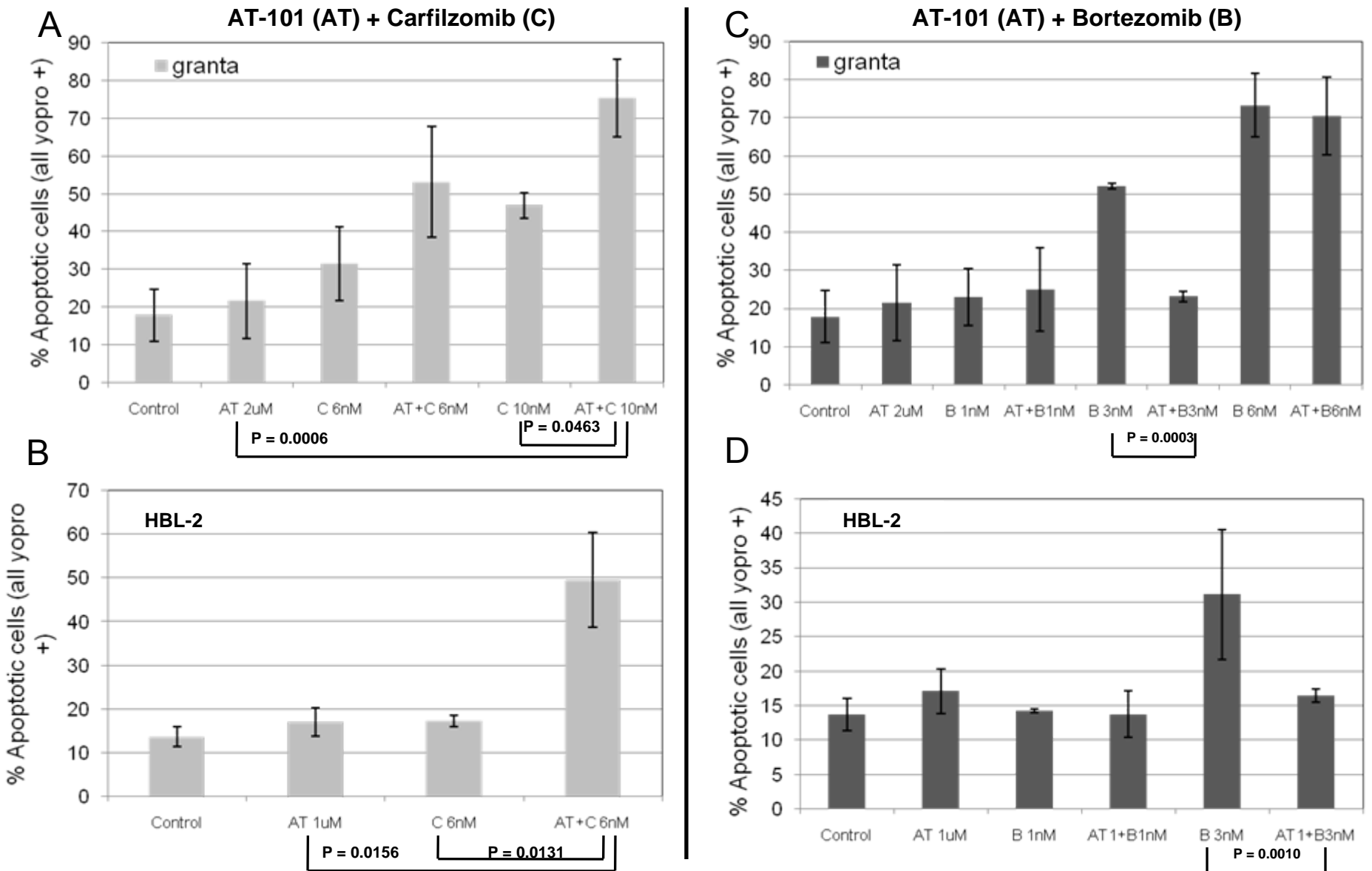
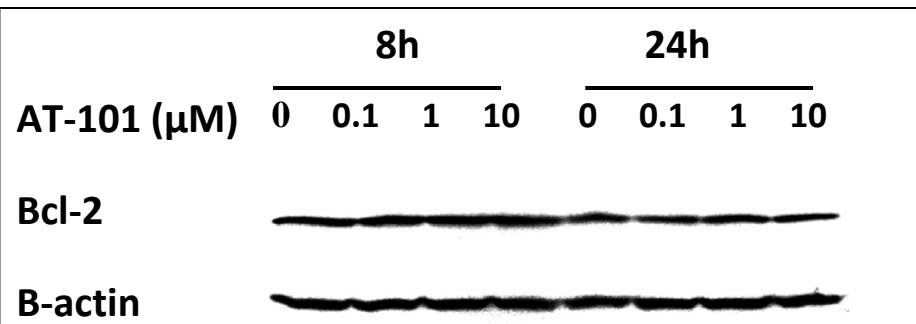
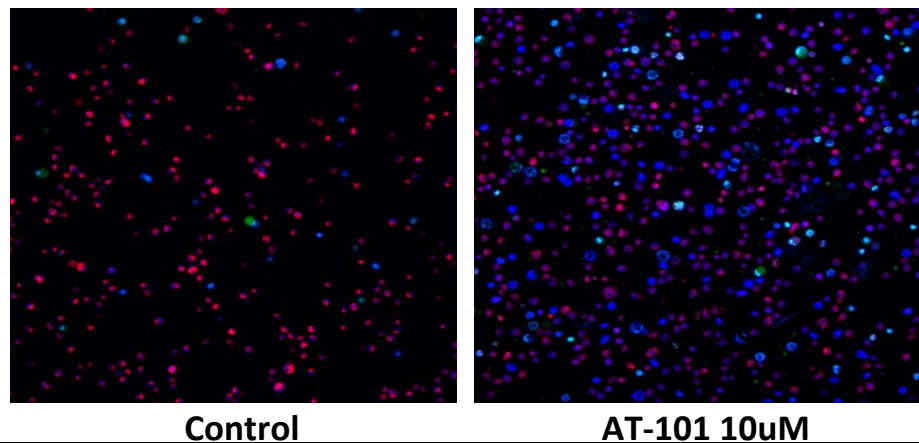
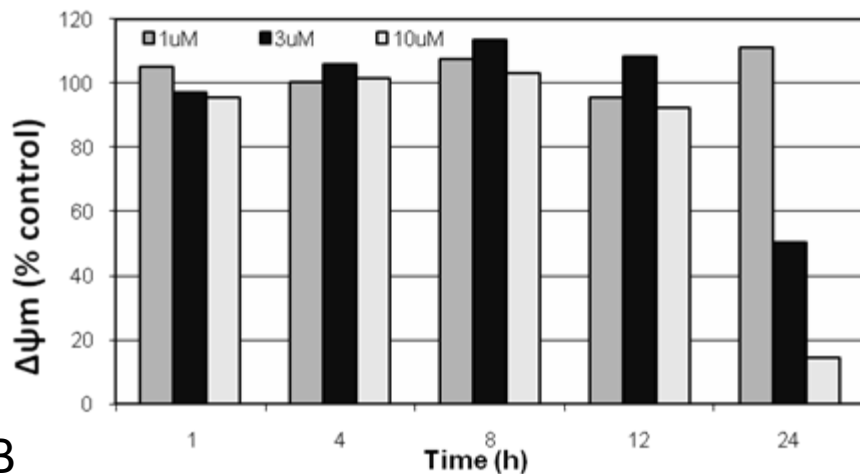


**Figure 3** Assessment of apoptosis by Yo-pro-1 and propidium iodide (PI) in HBL-2 and Granta cell lines. (A) and (B): Treatment with AT-101 (1 $\mu$ M or 2  $\mu$ M) and Carfilzomib (C, 6 nM or 10 nM) induces apoptosis in at least 50 % of cells ( $p \leq 0.0463$  for Granta and  $p \leq 0.0156$  for HBL-2). (C) and (D): The combination of AT-101 (1 $\mu$ M or 2  $\mu$ M) and bortezomib (1 nM, 3 nM, or 6 nM) may be antagonistic.



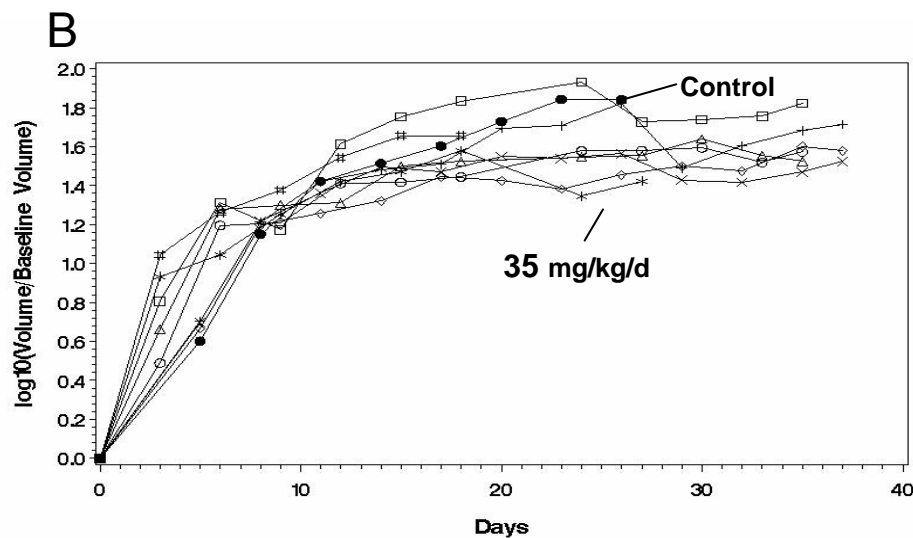
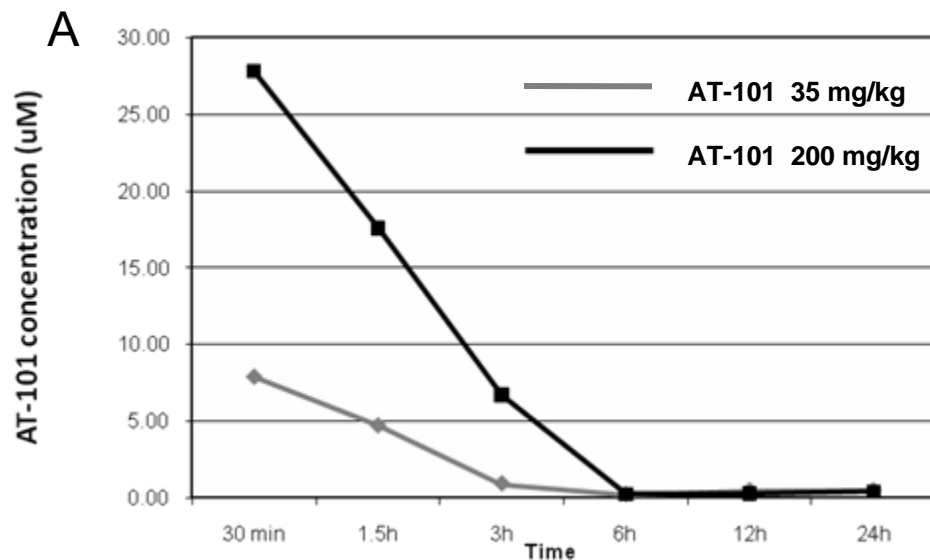
<b><u>SCHEDULES</u></b>		<b>T0</b>	<b>24h</b>	<b>48h</b>	<b>72h</b>
<b>I.</b>	<b>Simultaneous</b>	<b>AT-101</b>	→		
		<b>4-HC</b>	→		
<b>II.</b>	<b>24 h pre-Exposure</b>	<b>AT-101</b>	→		
		<b>4-HC</b>		→	
<b>III.</b>	<b>48 h pre-Exposure</b>	<b>AT-101</b>	→		
		<b>4-HC</b>			→

<b>Cell line</b>	<b>Schedule</b>	<b>AT-101 (uM)*</b>	<b>4-HC (uM) *</b>	<b>Combination Index</b>
<b>RL</b>	<b>I</b>	10	12	➤1
	<b>II</b>	5	12	0.6
	<b>III</b>	3.5	12	0.8

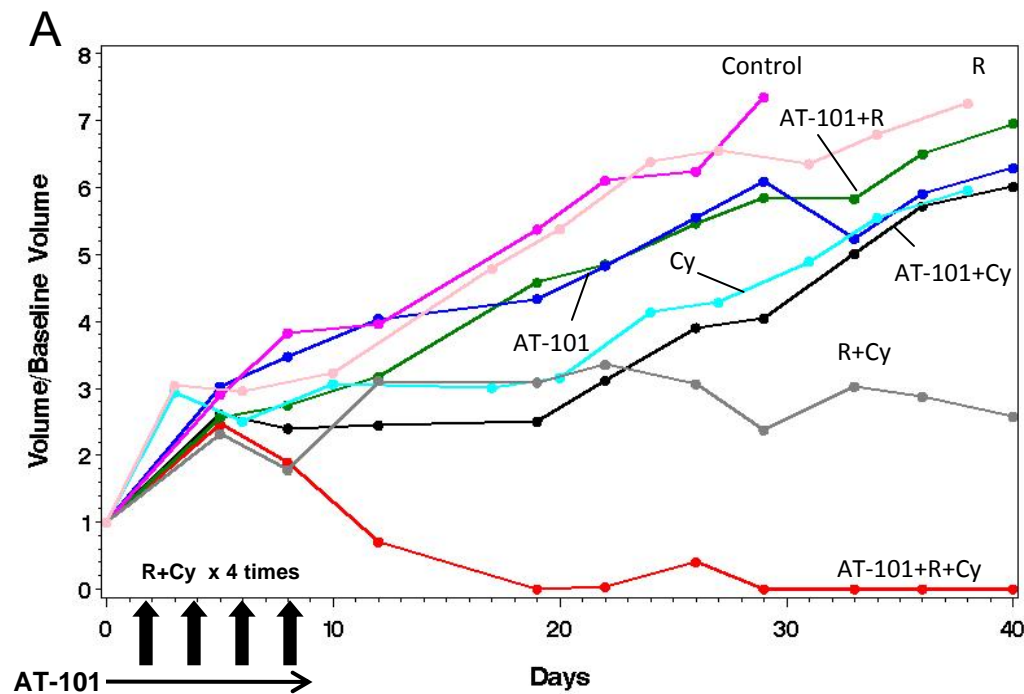
\* AT-101 and 4-HC concentrations represent the approximate IC<sub>60</sub> and IC<sub>30</sub> respectively.

**Figure 4** Diffuse Large-B cell line (RL) **(A)** Assessment of the mitochondrial membrane potential ( $\Delta\psi_m$ ). AT-101 (1  $\mu$ M, 3  $\mu$ M, 10  $\mu$ M) from 1 hour to 24 hours exposure **(B)** Confocal microscopy detection of apoptosis in a large B-cell lymphoma line (RL) treated with AT-101 for 24h. YO-PRO-1 (nuclei of apoptotic cells, green); Hoechst 33342 (nuclei, blue), MitoTracker Red (active mitochondria). AT-101 induces apoptosis in a large B-cell lymphoma cell line (RL) after exposure for 24h. Control, AR = 3%; AT-101 10  $\mu$ M, AT = 38.7% **(C)** Immunoblotting for Bcl-2 following treatment with AT-101 in a large B-cell lymphoma line (RL). AT-101 does not affect levels of Bcl-2. **(D)** Cytotoxicity assay for AT-101 combined with 4-HC in a large B-cell lymphoma line (RL). Model of in vitro exposure to AT-101 and other drugs; a pre-exposure to AT-101 for up to 48 hours before adding 4-HC for additional 24 hours revealed a synergistic interaction of the combination.



**Figure 5 In vivo SCID-beige xenograft model for DLBCL (RL)** (A) Pharmacokinetic (PK) modeling of AT-101 after a single administration by oral gavage. AT-101 was administered at a 35 mg/kg or a 200 mg/kg; the AT-101 peak plasma concentration was observed after 30 minutes of administration of the drug in both the dose levels, with the 200 mg/kg group showing a plasma average concentration almost four times greater than the 35 mg/kg group (7.88 µM and 27.78 µM respectively). After 24h, AT-101 was still detectable in plasma with average concentrations of 0.49 µM for the 35 mg/kg group and 0.39 µM for the 200 mg/kg. (B) In vivo activity of single AT-101 as a function of schedule. The 35 mg/kg/day for 14 days showed a statistically significant shrinkage of tumor volume compared to controls ( $p=0.008$ );  $p$  values are shown;  $p$  values for each treatment group compared to control. All significance testing is done at the  $p < 0.05$  level.  $N=5$  in each group.

Treatment 1	Treatment 2	p value
□ 100 mg/kg d 1,4,8,11	control	0.548
◇ 100 mg/kg/d x 3	control	1.000
○ 120 mg/kg d 1,4,8,11	control	0.095
△ 140 mg/kg d 1,4,8,11	control	0.151
+ 240 mg/kg/w	control	0.841
× 280 mg/kg/w	control	0.571
* 35 mg/kg/d	control	0.008
# 50 mg/kg/d	control	0.690



**B**

	AT-101 + Cy	AT-101 + R + Cy	AT-101 + R	AT-101	Cy	Control	R + C	R
AT-101 + Cy		0.0033	0.9993	0.9705	0.9998	0.9175	0.6958	0.7789
AT-101 + R + Cy	<b>0.0033</b>		<b>&lt;.0001</b>	<b>&lt;.0001</b>	<b>&lt;.0001</b>	<b>&lt;.0001</b>	<b>0.0341</b>	<b>&lt;.0001</b>
AT-101 + R	0.9993	<b>&lt;.0001</b>		0.9993	1.0000	0.9905	0.1816	0.9342
AT-101	0.9705	<b>&lt;.0001</b>	0.9993		0.9939	1.0000	0.0371	0.9980
Cy	0.9998	<b>&lt;.0001</b>	1.0000	0.9939		0.9594	0.1541	0.8247
Control	0.9175	<b>&lt;.0001</b>	0.9905	1.0000	0.9594		0.0174	0.9999
R + Cy	0.6958	0.0341	0.1816	0.0371	0.1541	0.0174		0.0047
R	0.7789	<b>&lt;.0001</b>	0.9342	0.9980	0.8247	0.9999	0.0047	

**Figure 6 In vivo SCID-beige xenograft model for DLBCL (RL) Combination experiments. (A)** The combination of oral AT-101 35 mg/kg/day for ten days regimen plus i.p. cyclophosphamide (Cy) and i.p. rituximab (R) in four administrations together on days 2, 4, 6, 8 showed significant tumor volume control compared to any other treatment group. **(B)** The multiple comparison analysis shows the superiority of the triplet combination to each other group ( $p \leq 0.0341$ ). Data represent p values for the comparisons. All significance testing is done at the  $p < 0.05$  level. N=7 in each group (n=6 in control group).